



**HAL**  
open science

## **Seed-free deposition of large-area adhesive diamond films on copper surfaces processed and patterned by femtosecond lasers**

Lisha Fan, Yunshen Zhou, Mengmeng Wang, Jean-François Silvain, Yongfeng Lu

### ► **To cite this version:**

Lisha Fan, Yunshen Zhou, Mengmeng Wang, Jean-François Silvain, Yongfeng Lu. Seed-free deposition of large-area adhesive diamond films on copper surfaces processed and patterned by femtosecond lasers. *Thin Solid Films*, 2017, 636, pp.499-505. <10.1016/j.tsf.2017.06.058>. <hal-01569398>

**HAL Id: hal-01569398**

**<https://hal.science/hal-01569398v1>**

Submitted on 11 Mar 2021

**HAL** is a multi-disciplinary open access archive for the deposit and dissemination of scientific research documents, whether they are published or not. The documents may come from teaching and research institutions in France or abroad, or from public or private research centers.

L'archive ouverte pluridisciplinaire **HAL**, est destinée au dépôt et à la diffusion de documents scientifiques de niveau recherche, publiés ou non, émanant des établissements d'enseignement et de recherche français ou étrangers, des laboratoires publics ou privés.



HAL Authorization

# Seed-Free Deposition of Large-Area Adhesive Diamond Films on Copper Surfaces Processed and Patterned by Femtosecond Lasers

*Lisha Fan<sup>a</sup>, Yun Shen Zhou<sup>a</sup>, Meng Meng Wang<sup>a</sup>, Jean-François Silvain<sup>b</sup>, and Yong Feng Lu<sup>a,\*</sup>*

<sup>a</sup> Department of Electrical and Computer Engineering, University of Nebraska, Lincoln, NE, 68588, USA

<sup>b</sup> Institut de Chimie de la Matière Condensée de Bordeaux – ICMCB-CNRS 87, Avenue du Docteur Albert Schweitzer, F-33608 Pessac Cedex, France

**Keywords:** diamond, copper, thin film, femtosecond laser processing

**Abstract:** We demonstrate that femtosecond (fs) laser patterning of Cu can be exploited to realize seed-free deposition of large-area adhesive diamond films on Cu. Fs-laser-induced nanostructures promote diamond nucleation density and result in diamond film formation within a laser fluence window from 2.6 to 3.6 J cm<sup>-2</sup>. Diamond films deposited on Cu surfaces prepared outside this window experience either complete film detachment or formation of low-quality ball-like diamond grains. Diamond/substrate interface roughness plays a critical role in controlling diamond quality and adhesion between substrates and diamond films. Large-area adhesive diamond films have been achieved on Cu substrate surfaces that were first modified with fs-laser irradiation and then scribed into grid patterns. The scribed channels function as expansion joints for stress relief. Strain-free diamond films have been achieved by optimizing the grid size. Using fs-laser processing for seed-free deposition of large-area diamond films on Cu is of great significance for diverse applications, such as thermal management and power electronic devices.

## 1. Introduction

Owing various great properties, diamond has long been envisioned as an ideal material for multiple applications, including but not limited to thermal management, electromechanical systems, wide band gap semiconductor, high-power-and-high-energy electronic devices, and quantum information processing [1-3]. Among various substrates used for diamond film deposition, Cu has been a promising one because of its technological importance in microelectronics and thermal management [4,5]. Take Cu heat sinks as an example, Cu has a medium thermal conductivity (TC,  $395 \text{ W m}^{-1} \text{ K}^{-1}$ ) and a large coefficient of thermal expansion (CTE,  $17 \times 10^{-6} \text{ K}^{-1}$ ) while diamond has a large TC ( $2200 \text{ W m}^{-1} \text{ K}^{-1}$ ) and a small CTE ( $1.5 \times 10^{-6} \text{ K}^{-1}$ ) [3]. Diamond coatings on Cu substrates with strong interfacial adhesion could provide a thermal conduction structure that exhibits a high TC for efficient heat dissipation and a moderate CTE adaptive to the Si/ceramic parts of microelectronic components, which could significantly increase the power density and prolong the lifetime of the devices [6].

Despite of the enormous potential in thermal management, large-area diamond films on Cu with strong adhesion have been proven extremely difficult [7, 8]. It is impeded by several major issues that interrelate with each other: 1) low diamond nucleation density, 2) poor diamond-Cu adhesion, and 3) diamond film cracking. The extremely low diamond nucleation density ( $5 \times 10^{-4} - 10^{-6} \mu\text{m}^{-2}$ ) is due to the poor affinity between Cu and carbon (C, diamond) [7]. A high-density nucleation must be achieved to produce continuous films. Diamond synthesis on Cu, which is unable to form carbide or to dissolve C, requires diamond seeds or surface defects to induce nucleation process by lowering the enthalpy change of nuclei formation [9]. Various surface modification approaches have been investigated to enhance the nucleation density, including

diamond seeding, ion implantation, interlayer addition, and diamond-Cu composite [10-19]. As a conventional solution, diamond seeding is performed by abrading a substrate surface by diamond powder in ultrasonic vibration to introduce scratches and grooves on substrate surfaces [16]. The diamond particles trapped inside the scratches and grooves provide sites for diamond growth. However, this technique produces random and non-uniform seed distribution, is short of reproducibility and nucleation density control [16]. A seedless surface treatment approach that provides precise control of the nucleation density is required.

An enhancement of the nucleation density is a necessary but not sufficient condition to achieve an adhesive diamond film on a Cu substrate. The non-carbide-forming nature of Cu leads to an abrupt mechanical interface and weak diamond-Cu adhesion. The largely different CTEs of diamond and Cu result in considerably high thermal stress in diamond film during the cooling process [3]. Even if continuous films could be grown on Cu, the high thermal stress addition to the abrupt diamond-Cu interfaces would cause destructive failure of the diamond films, such as film cracking and delamination [20-23]. Hartsell *et al* [11]. reported growth of continuous diamond films on scribed Cu surface. Fan *et al* [13, 17]. developed a two-step growth strategy to release trapped nucleation for producing large-area continuous diamond films. However, the diamond films obtained from the two independent works show weak adhesion to the substrates and can be easily peeled off [11, 13, 17]. Exploration of new interface design to produce adhesive diamond films on Cu is required.

In this study, we demonstrated a laser-enabled approach to addressing the challenges and successfully deposited large-area diamond films adhered to Cu substrates by precise control of

the interface roughness for mechanical interlocking and innovative design of “expansion joint” grid pattern for stress release. In our previous work, seed-free growth of diamond patterns have been realized by patterning silicon surface using fs lasers [24]. Laser-assisted combustion synthesis of diamond was described in our previous reports [24]. Prior to diamond deposition, an fs laser was used as irradiation source to process Cu substrates. Fs-laser-induced nanostructures promote nucleation density for the formation of continuous diamond films. Diamond films were obtained in a laser fluence window from 2.6 to 3.6 J cm<sup>-2</sup>. The films prepared outside this window suffer from either complete film detachment or formation of low-quality ball-like diamond grains. Surface roughness plays a critical role in controlling diamond quality and introducing mechanically adhesive interfaces between substrates and diamond films. The fs-laser-modified Cu surfaces were scribed into grid patterns for large-area adhesive diamond film deposition. The scribed channels function as expansion joints that absorb thermal expansion for effective stress relief. Residual stress analysis of diamond films deposited on the scribed Cu surfaces reveals that strain-free adhesive diamond films can be achieved by optimizing the grid size.

## **2. Experimental Details**

### **2.1 Fs laser processing of Cu substrates.**

A Ti:sapphire fs laser equipped with an amplifier (Legend F, Coherent Inc., central wavelength of 800 nm, pulse duration of 120 fs, and repetition rate of 1 kHz) was used for processing Cu substrates as shown in Fig. 1(a). An optical path consisting of an attenuator, a half-wave plate, and a polarizer was used to deliver the laser beam and tune the incident laser energy. The laser

beam was focused to a spot of 25  $\mu\text{m}$  in diameter. To investigate the diamond deposition on surfaces of different roughness, laser fluence was varied from 2.2 to 4.0  $\text{J}/\text{cm}^2$ . Surface scanning was performed with a scanning speed of 2.0  $\text{mm}/\text{s}$  and a line pitch of 10  $\mu\text{m}$ . For stress relief, deep channels were scribed on the fs-laser-modified Cu surfaces to form grid patterns with a scanning speed of 0.5  $\text{mm}/\text{s}$  and a laser fluence of 4.0  $\text{J}/\text{cm}^2$ . The Cu substrates scribed were ultrasonically cleaned to remove debris. Prior to diamond deposition, surface morphology and roughness of the Cu surfaces were characterized using a scanning electron microscope (SEM) and a 3D optical surface profiler.

## **2.2 Diamond growth on fs-laser-processed Cu substrates.**

Laser-assisted combustion chemical vapor deposition (CVD) of diamond was described in our previous reports [25, 26]. As shown in Fig.1(b), a gas mixture containing oxygen ( $\text{O}_2$ ), acetylene ( $\text{C}_2\text{H}_2$ ), and ethylene ( $\text{C}_2\text{H}_4$ ) with a volume ratio of 2:1:1 was used for diamond deposition. The wavelength of a wavelength-tunable carbon dioxide ( $\text{CO}_2$ ) laser was fixed at 10.532  $\mu\text{m}$  to resonantly excite the  $\text{CH}_2$ -wagging mode of the  $\text{C}_2\text{H}_4$  molecules. The substrate temperature was monitored using a noncontact pyrometer (Omega Engineering Inc., OS3752) and maintained at 730–750  $^\circ\text{C}$ . The distance between the substrate and the inner flame tip was kept to be around 0.5 mm. The microstructures of the diamond films were characterized using SEM. The crystalline quality and residual stress were analyzed using a confocal Raman microscope with a visible excitation radiation of a 514 nm continuous-wave (CW) laser.

## **3. Results and Discussion**

### **3.1 Fs laser surface nanostructuring of Cu**

Representative SEM images of surface structures of Cu substrates processed with the fs laser irradiation at different laser fluences are shown in Figs. 2(a)-(i). Strong dependence of surface topology on laser fluence was revealed. Large protrusions and valleys were observed in Cu surfaces modified at a laser fluence of  $4.0 \text{ J cm}^{-2}$  (Fig. 2(a)). The corresponding high-magnification SEM image (Fig. 2(j)) shows that the surface protrusions are composed of aggregation of densely packed nanoparticles of tens nanometers in diameter mainly due to re-deposition of ablated debris at a high laser fluence [27]. Irradiation at laser fluences in the middle range of  $3.0\text{-}3.6 \text{ J cm}^{-2}$  transforms the rough feature (Fig. 2(a)) to smooth structures with sparsely distributed ablated debris (Figs. 2(b)-(e)). At laser fluences in the range of  $2.2\text{-}2.8 \text{ J cm}^{-2}$ , the modified Cu surfaces exhibit periodic ripple patterns with a pitch size of around 400 nm in Figs. 2(f)-(i). The formation of surface periodic ripple patterns is often explained by spatial periodic energy distribution that is resulted from the interference between incident laser light with excited surface plasmon polaritons [28]. As the laser fluence decreases, the period of the ripple pattern becomes less regular. The surface nanostructures at two laser fluences,  $4.0$  and  $2.8 \text{ J cm}^{-2}$ , are compared in high-magnification SEM images (Figs. 2(j)-(k)). Compared with the rough Cu surface modified at a high fluence of  $4.0 \text{ J cm}^{-2}$ , the Cu surface modified at a lower fluence of  $2.8 \text{ J cm}^{-2}$  is much smoother with a ripple structure and sparsely scattered larger particles with diameters around 70 nm.

### **3.2 Diamond growth on the fs-laser-modified Cu substrates**

To investigate the influence of fs laser nanostructuring of Cu surfaces on diamond growth, the laser-modified Cu substrates were used for diamond growth by laser-assisted combustion flame CVD. This combustion CVD process is distinguished from physical vapor deposition (PVD)

because: 1) it starts from a mixture of precursor gases; and 2) diamond films form from the products generated from the combustion chemical reactions [29, 30]. Figure 3 shows the surface morphology of diamond films deposited on the fs-laser-modified Cu substrates at different laser fluences for 1 hr. As shown in low- and high-magnification SEM images (Figs. 3(a) and (j)), the film deposited on an fs-laser-modified Cu substrate at a laser fluence of  $4.0 \text{ J cm}^{-2}$  consists of ball-like diamond grains. According to the SEM image shown in Fig. 2(a), the Cu substrate modified at  $4.0 \text{ J cm}^{-2}$  exhibits a very rough feature consisting of large protrusions and valleys. The protrusions on the rough surface were surrounded by the flame and the heat dissipation at the protrusions was reduced, leading to higher local temperatures than well faceted diamond growth window ( $760\text{-}780 \text{ }^\circ\text{C}$ ) to form ball-like diamond grains.

Without any diamond seeding process, diamond films were formed on fs-laser-modified Cu substrates at fluences below  $3.6 \text{ J cm}^{-2}$ , although films prepared at fluences below  $2.6 \text{ J cm}^{-2}$  encountered complete film detachment as soon as removing them from the flame. High-magnification SEM image in Fig. 3(k) shows that a continuous diamond film with well faceted diamond grains formed on an fs-laser-modified Cu substrate at a laser fluence of  $2.8 \text{ J cm}^{-2}$ . The corresponding Cu surface modified is composed of periodic ripple patterns with sparsely scattered spherical particles as shown in Fig. 2(k).

The formation of diamond films on fs-laser-modified Cu substrates is attributed to enhanced nucleation density on fs-laser-induced nanostructures. Short-time diamond growth on the Cu surfaces processed at a laser fluence of  $2.8 \text{ J cm}^{-2}$  was performed to evaluate the nucleation density. Figures 4(a)-(b) show the surface morphology of the Cu surfaces after 10 and 15 min

diamond growth, respectively. In Fig. 4(a), spherical diamond nuclei with size around 200 nm are sparsely scattered over the Cu surface formed after 10 min deposition. After 15 min deposition, faceted diamond particles with a size around 500 nm are embedded inside a Cu “silk” matrix as shown in Fig. 4(b). Compared with the reported nucleation density in the range of  $10^{-4}$ - $10^{-6} \mu\text{m}^{-2}$  [7], the diamond films prepared on the fs-laser-modified Cu surface exhibit a much higher nucleation intensity of  $1.3 \mu\text{m}^{-2}$ , suggesting the critical role of the fs laser surface modification in enhancing diamond nucleation. Preferential nucleation on defects that protrude from the surfaces, such as etch pits/craters, edges, scratches, and whiskers, has been demonstrated by several research groups [31-33]. Enhanced diamond nucleation density on defects can be attributed to following reasons: 1) presence of abundant dangling bonds aiding the chemisorption of reactive species; 2) increased reactant flux at the protrusions and edges, and 3) minimization of interfacial energy by forming diamond nuclei at the prominent tips [34]. The surface nanostructures formed with fs laser irradiation introduce high density of defects in the Cu surface, which is favorable for high density diamond nucleation and subsequently contributes to the formation of continuous diamond thin films.

However, an increase in nucleation density alone does not guarantee better adhesion because no carbide formation at the interface leads to a weak and abrupt mechanical interface between Cu and diamond. Due to the largely different CTEs between diamond and Cu, considerably high thermal stress that builds up between diamond films and Cu substrates ultimately leads to film deformation, even cracking, as cooling down the diamond films from high growth temperature to room temperature. Film cracking was observed in diamond films prepared on fs-laser-modified Cu substrates within a narrow laser fluence window from 2.6 to 3.6  $\text{J cm}^{-2}$  in Figs. 3(b)-(g).

Diamond films on Cu surfaces processed at even lower laser fluences completely detached from the processed Cu substrates, leaving the Cu surfaces exposed as shown in Figs. 3(h)-(i).

Generally, there are three different mechanisms contributing to the film-substrate adhesion: 1) mechanical interlocking, 2) physisorption, and 3) chemisorption [35-38]. Chemisorption involves interchange of electrons and formation of chemical bonding [36]. Due to the non-carbide-forming nature of Cu, chemisorption can be ruled out for the interaction between diamond films and Cu substrates. Physisorption or intermolecular interactions are based on the electrostatic forces or Van der Waals forces [39-41]. However, both types of interactions are short ranged with the interaction distance in the atomic radius scale ( $< 1$  nm) [36]. Large gaps with sizes of around hundred nanometers present at the boundaries between diamond crystals and Cu matrix is out of the interaction range of physisorption. Diamond nuclei embedded in Cu, acting like anchors, is a typical characteristic of mechanical interlocking [36]. Therefore, the adhesion between diamond films and Cu substrates primarily depends on the mechanical interlocking, which is mainly related to the substrate surface roughness. A 3D optical profiler was thus used to analyze the surface roughness,  $S_z$ , of the Cu substrates modified at different laser fluences. Figure 5(a) shows a representative 2D surface profile of an fs-laser-modified Cu surface at a laser fluence of  $4.0 \text{ J cm}^{-2}$ . The surface roughness is the arithmetic average of the absolute values of the 2D profile height deviation from the mean line, which was plotted as a function of the laser fluence in Fig. 5(b), showing an exponential increase with the laser fluence. The surface roughness increases slowly with the laser fluence below  $3.6 \text{ J cm}^{-2}$ , but rises up rapidly as the laser fluence increases further. Correlating the surface roughness curve with the diamond growth, it is noticed that film detachment became significant on Cu surfaces with a

surface roughness below 1.5  $\mu\text{m}$ . The film detachment on a smoother surface can be related to the weaker mechanical interlocking between the films and the substrates [35].

The diamond quality was evaluated by Raman spectroscopy using a visible 514 nm CW laser as the excitation source. Figure 5(c) shows a Raman spectrum of a diamond film grown on a Cu substrate processed at a laser fluence of 4.0 J cm<sup>-2</sup>. The diamond peak at 1332 cm<sup>-1</sup> and non-diamond bands (G-band, D1 and D2 bands) located at 1240, 1350, and 1500 cm<sup>-1</sup>, respectively, were resolved through curve fitting the Raman spectrum. Diamond quality index factor,  $Q$ , was retrieved using Equation (1),

$$Q = \frac{I_D}{\left(I_D + \frac{I_G}{233}\right)} 100\% , \quad (1)$$

where  $I_D$  and  $I_G$  are the intensity of the diamond peak and total intensity of the non-diamond peaks, respectively [42]. The diamond quality index factors were plotted as a function of the surface roughness of the fs-laser-modified Cu substrates in Fig. 5(d). A strong dependence of the diamond quality on the surface roughness was extracted. With a surface roughness below 2  $\mu\text{m}$  (laser fluence below 3.6 J cm<sup>-2</sup>), the diamond quality index factors are over 95%. However, it drops rapidly as the surface roughness increases over 2  $\mu\text{m}$  (laser fluence above 3.6 J cm<sup>-2</sup>), suggesting a considerable amount of graphitic carbon in the films. This is consistent with the observation shown in Figs. 3(j)-(k). Well faceted diamond grains were observed at a low laser fluence of 2.8 J cm<sup>-2</sup> while ball-like diamond grains were observed at a high laser fluence of 4.0 J cm<sup>-2</sup>.

### 3.3 Diamond growth on the fs-laser-modified Cu substrates

Although rough diamond/Cu interfaces provide better mechanical interlocking between the diamond films and the substrates to some extent, the diamond films on Cu surfaces processed within the laser fluence window from 2.6 to 3.6 J cm<sup>-2</sup> are just weakly bonded with the Cu substrates as shown in Fig. 3. To produce large-area adhesive diamond films, the fs-laser-modified Cu surfaces were subsequently scribed into micro-size grid patterns using a high laser power and a slow scanning speed. Large-area adhesive diamond films were obtained without any film cracking. This ideal was inspired by the expansion joints that are widely employed in concrete road construction for releasing thermal expansion among joined concrete squares. Figures 6(a)-(b) show an fs-laser-scribed Cu surface with a grid size of 50 μm. The high-magnification image (Fig. 6(b)) shows that the scribed channel has a depth of ~10 μm and a width of ~5 μm. Figure 6(c) shows a low-magnification SEM image of the surface morphology of a diamond film deposited on the Cu surface scribed. No film detachment or cracking occurred in the diamond film. As shown in a high-magnification image of the diamond film in Fig. 6(d), diamond film in each square tends to squeeze with surrounding squares when it grows thicker due to relaxation of thermal stress. Diamond has a lower CTE than Cu, compressive thermal stress is thus formed in the diamond film during the cooling process. The shape deformation indicates that the scribed channels effectively absorb the thermally induced volume change during the cooling process for stress relief.

The influence of the grid size on the diamond growth, especially residual stress release, was investigated. Raman spectroscopy was used to measure the residual stress existing in the diamond films through the Raman peak shift. A strain-free diamond film has the signature Raman peak located at 1332 cm<sup>-1</sup>. A compressive or tensile stress induces a shift of the diamond

peak to higher or lower wavenumbers, respectively [43]. Residual stress in a diamond film consists of two major parts as expressed in Equation (2),

$$\sigma_{residual} = \sigma_{thermal} + \sigma_{intrinsic}. \quad (2)$$

One is the thermal stress, which is compressive and caused by the mismatch of the CTEs between diamond and substrate material and developed during the cooling process from the high growth temperature. The other one is the intrinsic stress which is a cumulative result of grain boundary formation and impurities incorporation into the film during deposition, which is often revealed to be tensile.

The residual stress in diamond films was estimated from the Raman peak shift value,  $\Delta\nu$ , using the following expression based on a general model developed by Ager and Drory [44]:

$$\sigma_{residual} = -0.567 \times (\nu_m - \nu_0), \quad (3)$$

where  $\nu_m$  is the peak position observed and  $\nu_0$  is the Raman peak of a strain-free diamond film ( $1332 \text{ cm}^{-1}$ ). Therefore, if  $\nu_m < \nu_0$ , the residual stress is tensile ( $\sigma_{residual} > 0$ ) and compressive ( $\sigma_{residual} < 0$ ) if  $\nu_m > \nu_0$ . The Raman peak shift values were retrieved by averaging over a  $200 \times 200 \text{ }\mu\text{m}^2$  Raman mapping of the diamond peak position of diamond films on the Cu surfaces scribed as shown in the inset of Fig. 6(e). The diamond Raman peak shift and the calculated residual stress were plotted as a function of the grid size in Fig. 6(e). The residual stress transforms from compressive to tensile type as the grid size increases. Diamond films with the lowest stress were obtained on scribed Cu surfaces with a grid size of  $50 \text{ }\mu\text{m}$ . The diamond film on a Cu surface scribed with a grid size of  $25 \text{ }\mu\text{m}$  experiences a compressive stress. The compressive stress indicates that the diamond film is well bonded to the substrate and experiences the thermally induced compressive stress. Diamond films on Cu surfaces scribed

with grid sizes of 75-200  $\mu\text{m}$  exhibit intrinsic defect-induced tensile stress. As shown in Fig. 7, film delamination was observed in the diamond films on Cu substrates scribed with grid sizes of 150 and 200  $\mu\text{m}$ . The film delamination and the intrinsic defect-induced tensile stress indicate that these films are just weakly bonded with the substrates. By optimizing the grid size, the thermally induced compressive stress can be properly released through the scribing channels and compensated with the defect-induced tensile stress, leading to a strain-free diamond film with a grid size of 50  $\mu\text{m}$ . Diamond films with an area size of 0.5  $\text{cm}^2$  were obtained. It is demonstrated that the fs-laser scribing process leads to an optimization of stress release through elastic relaxation in the diamond films.

#### **4. Conclusion**

In summary, fs laser processing was used for deposition of large-area adhesive diamond film without using a diamond seeding process. The surface nanostructures and moderate roughness induced by the fs laser irradiation lead to enhanced diamond nucleation and improved mechanical interlocking at the interfaces between the substrates and the diamond films. The fs-laser-modified Cu surface was scribed into grid patterns for thermal stress relief, on which large-area adhesive diamond films were formed. Residual stress of the deposited films was evaluated using Raman spectroscopy. The diamond film on Cu surfaces scribed with a grid size of 50  $\mu\text{m}$  exhibits a strain free feature. Such adhesive diamond films on Cu substrates offer high thermal conductivity, promising for applications in many fields, such as thermal management and power electronics.

#### **Author Contributions**

The manuscript was written through contributions of all authors. All authors have given approval to the final version of the manuscript. These authors, Lisha Fan, Yun Shen Zhou, and Meng Meng Wang, contributed equally to this manuscript. Drs. Lisha Fan and Yun Shen Zhou composed the manuscript, prepared the figures, and conducted data analysis & discussion. Mr. Meng Meng Wang contributed to the experiments and data collection. Dr. Jean-François Silvain provided essential information on thermal stress analysis and diamond-Cu adhesion. Dr. Yong Feng Lu is the corresponding author who supervised the project and conceived the ideas.

### **Funding Sources**

This work was supported by National Science Foundation [grant numbers CMMI 1265122]; and Nebraska Center for Energy Sciences Research (NCEsr).

### **Acknowledgements**

The authors gratefully appreciate the financial supports from National Science Foundation (CMMI 1265122) and Nebraska Center for Energy Sciences Research (NCEsr). In addition, the authors would like to express our appreciation towards Dr. D. R. Alexander in the Department of Electrical & Computer Engineering at the University of Nebraska-Lincoln for providing convenient access to the SEM.

## References

- [1] M. Schwander, K. Partes, A review of diamond synthesis by CVD processes, *Diam. Relat. Mater.* 20 (2011) 1287-1301.
- [2] M. N. R. Ashfold, P. W. May, C. A. Rego, Thin film diamond by chemical vapor deposition methods, *Chem. Soc. Rev.* 23 (1994) 21-30.
- [3] J. Asmussen, D. K. Reinhard, *Diamond Films Handbook*, Merceel Dekker, New York, 2002, pp. 511-535.
- [4] B. Q. Wan, X. Y. Sun, H. T. Ma, R. F. Feng, Y. S. Li, Q. Yang, Plasma enhanced chemical vapor deposition of diamond coatings on Cu-W and Cu-WC composites, *Surf. Coat. Technol.* 284 (2015) 133-138.
- [5] A. M. Abyzov, S. V. Kidalov, F. M. Shakhov, High thermal conductivity composite of diamond particles with tungsten coating in a copper matrix for heat sink application, *Appl. Therm. Eng.* 48 (2012) 72-80.
- [6] K. Yosida, H. Morigami, Thermal properties of diamond/copper composite material, *Microelectron. Reliab.* 44 (2004) 303-308.
- [7] L. Constant, C. Speisser, F. Le Normand, HFCVD diamond growth on Cu(111) Evidence for carbon phase transformations by in situ AES and XPS, *Surf. Sci.* 387 (1997) 28-43.
- [8] S. Ojika, S. Yamashita, K. Kataoka, T. Ishikura. Diamond grain growth on Cu substrate, *Jpn. J. Appl. Phys.* 32 (1993) L1681-L683.
- [9] J. C. Arnault, L. Demuyneck, C. Speisser, F. Le Normand, Mechanisms of CVD diamond nucleation and growth on mechanically scratched Si(100) surfaces, *Eur. Phys. J. B* 11 (1999) 327-343.

- [10] M. Chandran, C. R. Kumaran, S. Vijayan, S. S. Bhattacharya, M. S. Ramachandra Rao, Adhesive microcrystalline diamond coating on surface modified non-carbide forming substrate using hot filament CVD, *Mater. Express* 2 (2012) 115-120.
- [11] M. L. Hartsell, L. S. Plano, Growth of diamond films on copper, *J. Mater. Res.* 9 (1994) 921-926.
- [12] T. P. Ong, F. Xiong, R. P. H. Chang, Mechanism for diamond nucleation and growth on single crystal copper surfaces implanted with carbon, *Appl. Phys. Lett.* 60 (1992) 2083-2085.
- [13] Q. H. Fan, E. Pereira, J. Gracio, Diamond deposition on copper: studies on nucleation, growth, and adhesion behavior, *J. Mater. Sci.* 34 (1999) 1353-1365.
- [14] L. Constant, F. Le Normand, HFCVD diamond nucleation and growth on polycrystalline copper: kinetic study, *Thin Solid Films*, 516 (2008) 691-695.
- [15] Z. Ma, J. Wang, Q. Wu, C. Wang, Preparation of flat adherent diamond films on thin copper substrates using a nickel interlayer, *Surf. Coat. Technol.* 155 (2002) 96-101.
- [16] N. Ali, Q. H. Fan, W. Ahmed, I.U. Hassan, C. A. Rego, I. P. O'Hare, Role of surface pre-treatment in the CVD of diamond films on copper, *Thin Solid Films* 355-356 (1999) 162-166.
- [17] Q. H. Fan, J. Gracio, E. Pereira, Free-standing film preparation using copper substrate, *Diam. Relat. Mater.* 6 (1997) 422-425.
- [18] X. Liu, Q. Wei, Z. Yu, D. Yin, CVD diamond film deposited on copper substrate enhanced by a thin platinum modification layer, *Phys. Status Solidi A.* 11 (2012) 2217-2222.
- [19] Y. X. Han, H. Ling, J. Sun, M. Zhao, T. Gebre, Enhanced diamond nucleation on copper substrates by graphite seeding and CO<sub>2</sub> laser irradiation, *Appl. Surf. Sci.* 254 (2008) 2054-2058.

- [20] W. Q. Qiu, Z.W. Liu, L. X. He, D. C. Zeng, Y. W. Mai, Improved interfacial adhesion between diamond film and copper substrate using a Cu(Cr)-diamond composite interlayer, *Mater. Lett.* 81 (2012) 155-157.
- [21] S. A. Catledge, Y. K. Vohra, Adhesion of nanostructured diamond film on a copper-beryllium alloy, *J. Mater. Res.* 23 (2008) 2373-2381.
- [22] N. Ali, W. Ahmed, C. A. Rego, Q. H. Fan, Chromium interlayer as a tool for enhancing diamond adhesion on copper, *Diam. Relat. Mater.* 9 (2000) 1464-1470.
- [23] N. Jiang, L. C. Wang, J. H. Won, M. H. Jeon, Y. Mori, A. Hatta, T. Ito, T. Sasaki, A. Hiraki, Interfacial analysis of CVD diamond on copper substrate, *Diam. Relat. Mater.* 6 (1997) 743-746.
- [24] M. Wang, Y. S. Zhou, Z. Q. Xie, Y. Gao, X. N. He, L. Jiang, Y. F. Lu, Seed-free growth of diamond patterns on silicon predefined by femtosecond laser direct writing, *Cryst. Growth Des.* 13 (2013) 716-722.
- [25] L. Fan, Y. S. Zhou, M. X. Wang, Y. Gao, L. Liu, J. F. Silvain, Y. F. Lu, Resonant vibrational excitation of ethylene molecules in laser-assisted diamond deposition, *Laser Phys. Lett.* 11 (2014) 076002.
- [26] L. Fan, Z. Q. Xie, J. B. Park, X. N. He, Y. S. Zhou, L. Jiang, Y. F. Lu, Synthesis of nitrogen-doped diamond films using vibrational excitations of ammonia molecules in laser-assisted combustion flames, *J. Laser Appl.* 24 (2012) 022001.
- [27] A. Y. Vorobyev, C. Guo, Enhanced absorptance of gold following multipulse femtosecond laser ablation, *Phys. Rev. B* 72 (2005) 195422.
- [28] A. Y. Vorobyev, C. Guo, Direct femtosecond laser surface nano/microstructuring and its applications, *Laser Photonics Rev.* 7 (2013) 385-407.

- [29] L. Li, C. Xu, Y. Zhao, K. J. Ziegler, Balancing surface area with electron recombination in nanowire-based dye-sensitized solar cells, *Sol. Energ.* 132 (2016) 214-220.
- [30] L. Li, S. Chen, J. Kim, C. Xu, Y. Zhao, K. J. Ziegler, Controlled synthesis of tin-doped indium oxide (ITO) nanowires, *J. Cryst. Growth* 413 (2015) 31-36.
- [31] R. Polini, Diamond nucleation on cleaved Si(111), *J. Appl. Phys.* 72 (1992) 2517-2519.
- [32] R. Ramesham, C. Ellis, Selective growth of diamond crystals on the apex of silicon pyramids, *J. Mater. Res.* 7 (1992) 1189-1194.
- [33] E. I. Givargizov, L. L. Aksenova, A. V. Kuznetsov, P. S. Plekhanov, E. V. Rakova, A. N. Stepanova, V. V. Zhirnov, P. C. Nordine, Growth of diamond particles on sharpened silicon tips for field emission, *Dia. Related Mater.* 5 (1996) 938-942.
- [34] P. A. Denning, D. A. Stevenson, Influence of substrate topography on the nucleation of diamond thin films, *Appl. Phys. Lett.* 59 (1991) 1562-1564.
- [35] Y. Y. Wang, C. J. Li, A. Ohmori, Influence of substrate roughness on the bonding mechanisms of high velocity oxy-fuel sprayed coatings, *Thin Solid Films* 485 (2005) 141-147.
- [36] R. E. Clausing, L. L. Horton, J. C. Angus, P. Koidl, *Diamond and diamond-like films and coatings*, Plenum Press, New York and London, pp. 411-414.
- [37] K. L. Mittal, Adhesion measurement of films and coatings, *Electrocompo. Sci. Tech.* 3 (1976) 21-42.
- [38] L. H. Lee, New perspectives in polymer adhesion mechanisms – importance of diffusion and molecular bonding in adhesion, *Proc. of SPIE* 1999 (1993) 6-21.

- [39] Y. Zhao, J. G. Clar, L. Li, J. Xu, T. Yuan, J. C. J. Bonzongo, K. J. Ziegler, Selective desorption of high purity (6,5) SWCNTs from hydrogels through surfactant modulation, *Chem. Commun.* 52 (2016) 2928-2931.
- [40] J. G. Clar, T. Yuan, Y. Zhao, J. C. J. Bonzongo, K. J. Ziegler, Evaluation of critical parameters in the separation of single wall carbon nanotubes through selective adsorption onto hydrogels, *J. Phys. Chem. C*, 118 (2014) 15495-15505.
- [41] J. G. Clar, C. A. S. Batista, S. Youn, J. C. J. Bonzongo, K. J. Ziegler, Interactive forces between sodium dodecyl sulfate-suspended single-walled carbon nanotubes and agarose gels, *J. Am. Chem. Soc.* 135 (2013) 17758-17767.
- [42] G. W. Bak, K. Fabisiak, L. Klimek, M. Kozanecki, E. Staryga, Investigation of biaxial stresses in diamond films deposited on a silicon substrate by the HFCVD method, *Opt. Mater.* 30 (2008) 770-773.
- [43] T. Guillemet, A. Kusaik, L. Fan, J. M. Heintz, N. Chandra, Y. S. Zhou, J. F. Silvain, Y. F. Lu, J. L. Battaglia, Thermal characterization of diamond films through modulated photothermal radiometry, *ACS Appl. Mater. Interfaces*, 6 (2014) 2095-2102.
- [44] J. W. Ager, M. D. Drory, Quantitative measurement of residual biaxial stress by Raman spectroscopy in diamond grown on a Ti alloy by chemical vapor deposition, *Phys. Rev. B* 48 (1993) 2601-2607.

## List of Figure Captions

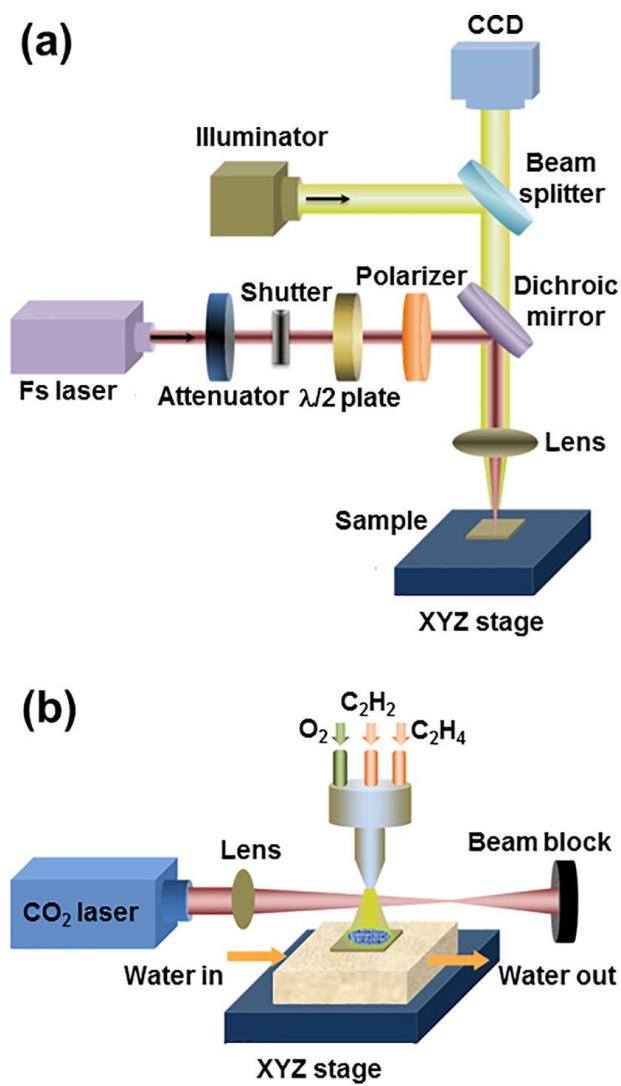


**Figure 1.** (Color online) Schematic setups of (a) an fs laser processing system and (b) a laser-assisted combustion CVD system.

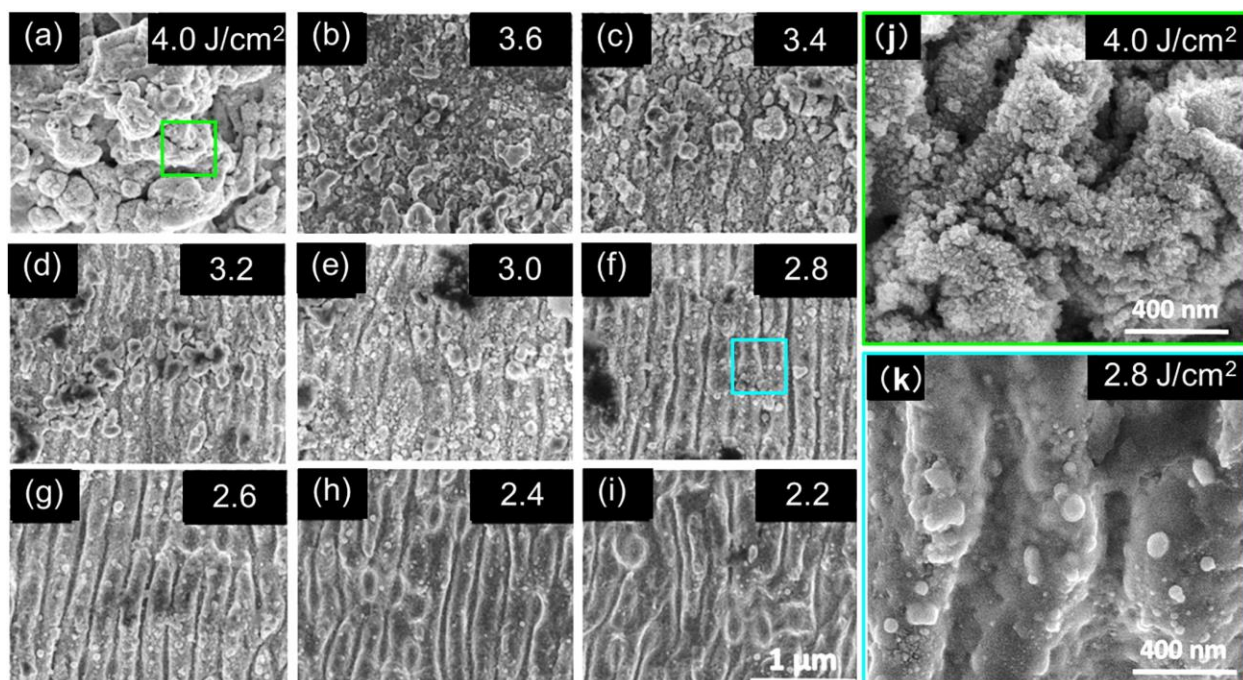


**Figure 2.** (Color online) (a)-(i) Low- and (j)-(k) high-magnification SEM images of the fs-laser-modified Cu surfaces at different laser fluences.

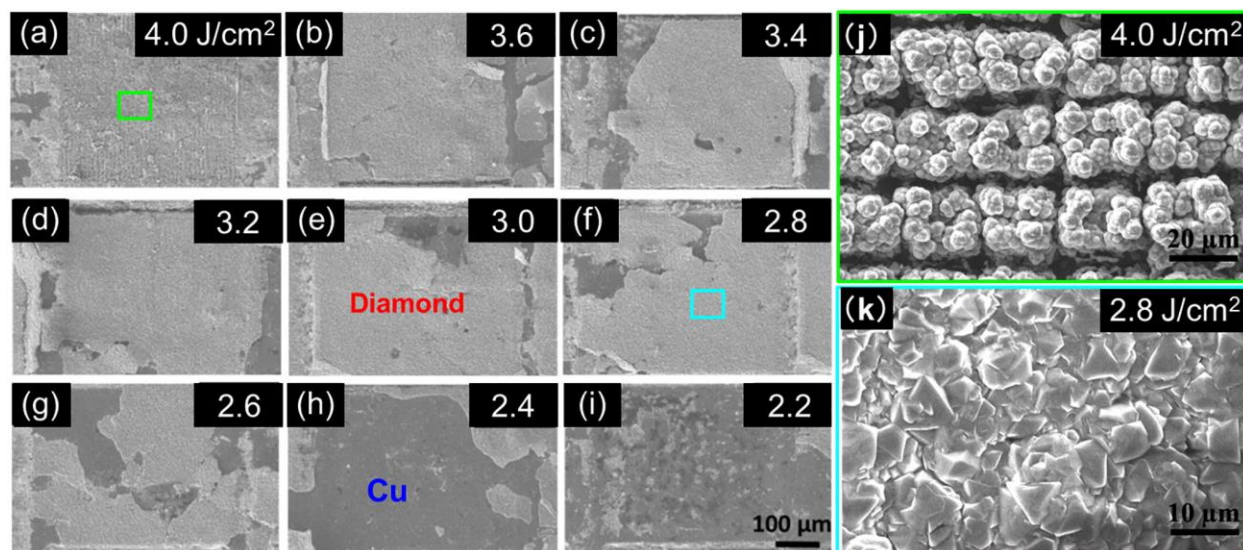


**Figure 3.** (Color online) (a)-(i) Low- and (j)-(k) high-magnification SEM images of diamond films deposited on fs-laser-modified Cu substrates for 1 hr growth.

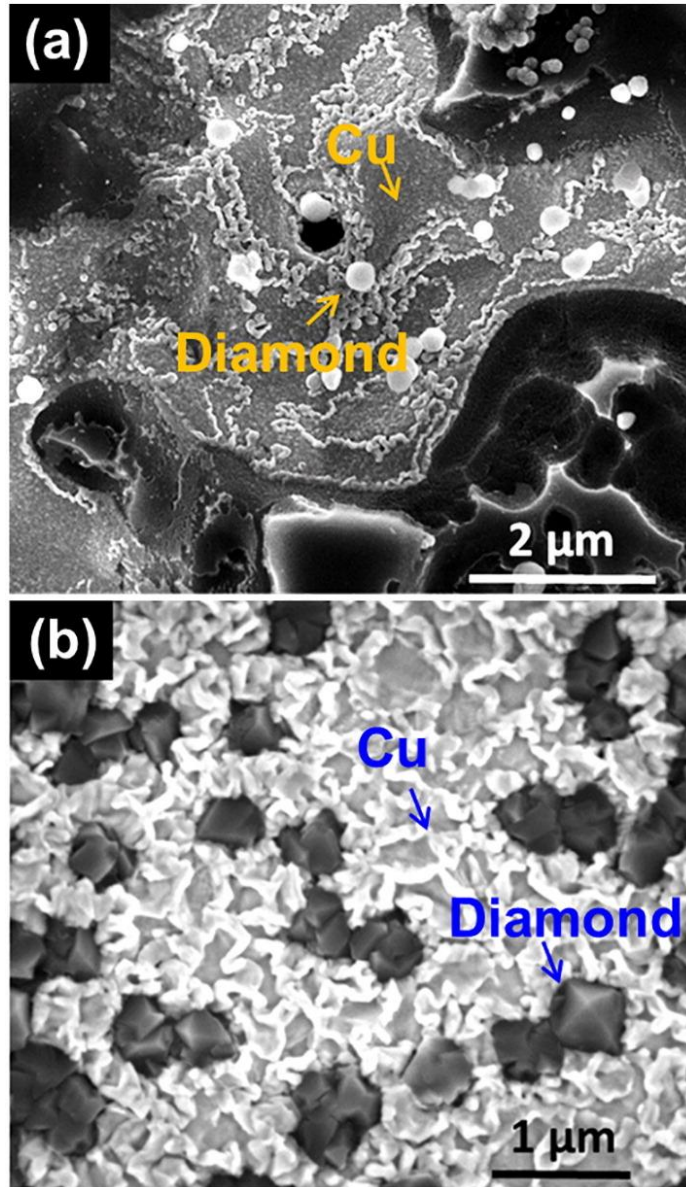


**Figure 4.** (Color online) SEM images of the Cu surfaces after diamond deposition for (a) 10 and (b) 15 min.

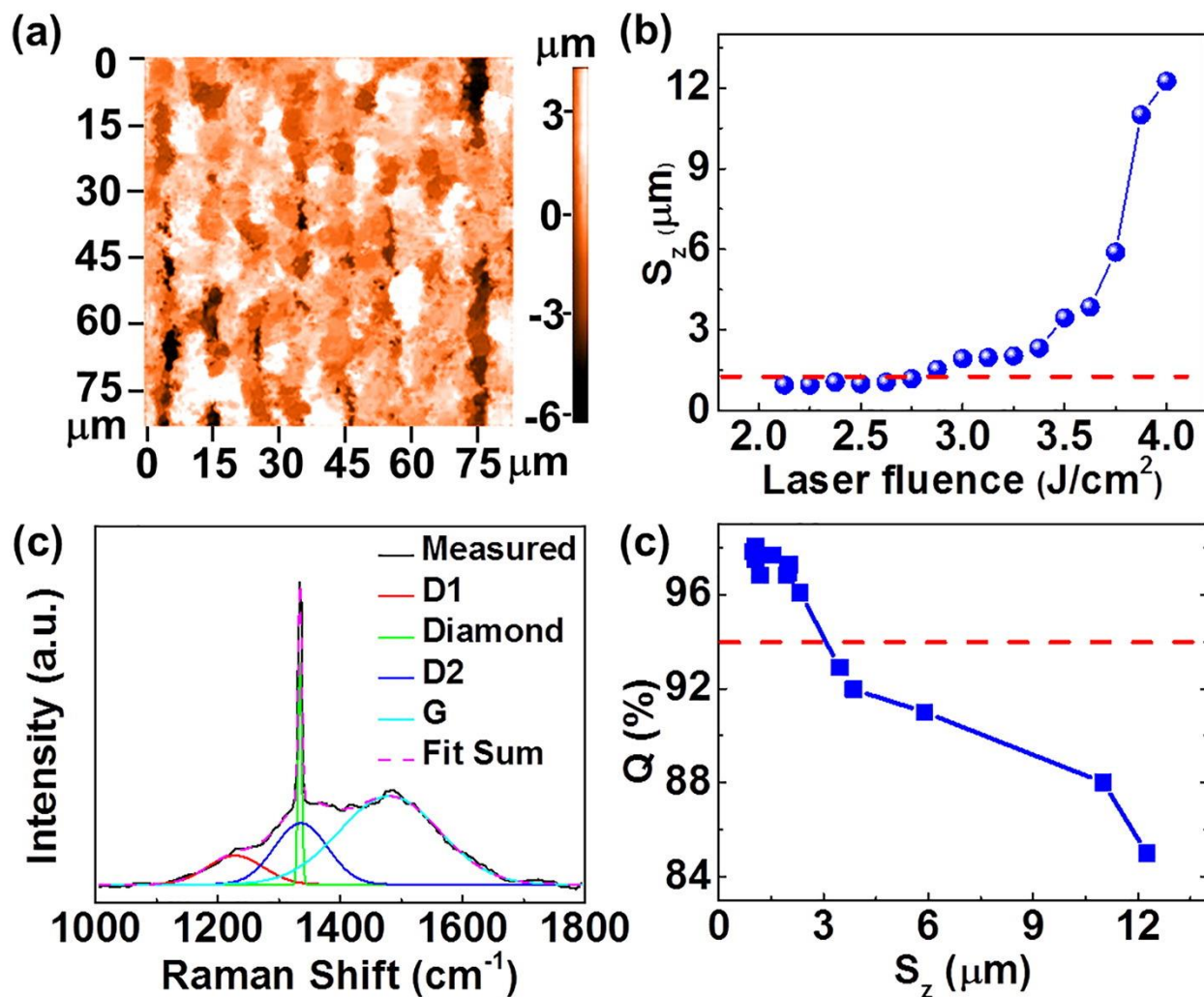


**Figure 5.** (Color online) (a) A 2D optical surface profile of an fs-laser-modified Cu surface at a laser fluence of  $4.0 \text{ J cm}^{-2}$ ; (b) The surface roughness plotted as a function of the laser fluence; (c) a Raman spectrum of a diamond film deposited on an fs-laser-modified Cu surface at a laser fluence of  $4.0 \text{ J cm}^{-2}$ ; (d) The diamond quality index factor plotted as a function of the surface roughness.

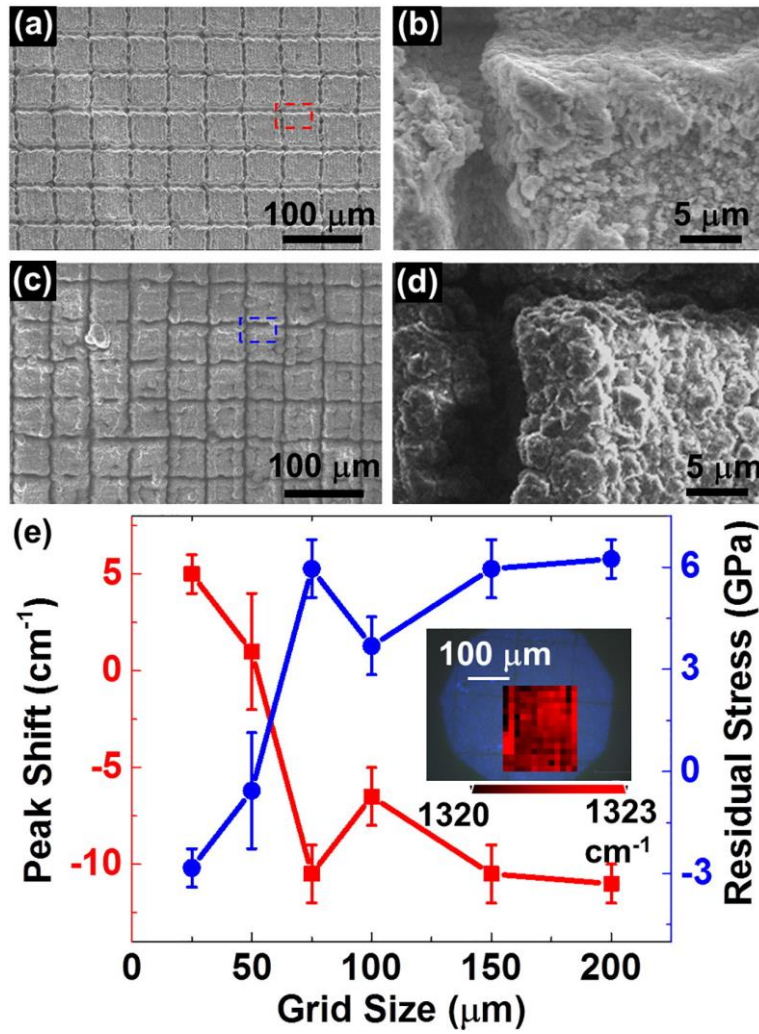


**Figure 6.** (Color online) (a) Low- and (b) high-magnification SEM images of an fs-laser-scribed Cu surface with a grid size of 50  $\mu\text{m}$ . (c) Low- and (d) high-magnification SEM images of a large-area diamond film on the fs-laser-scribed Cu substrate after 3 hr deposition. (e) The diamond Raman peak shift (red square) and residual stress (blue circle) plotted as a function of the grid size. The inset of (e) is a Raman mapping of the diamond peak position of a diamond film deposited on an fs-laser-scribed Cu surface.

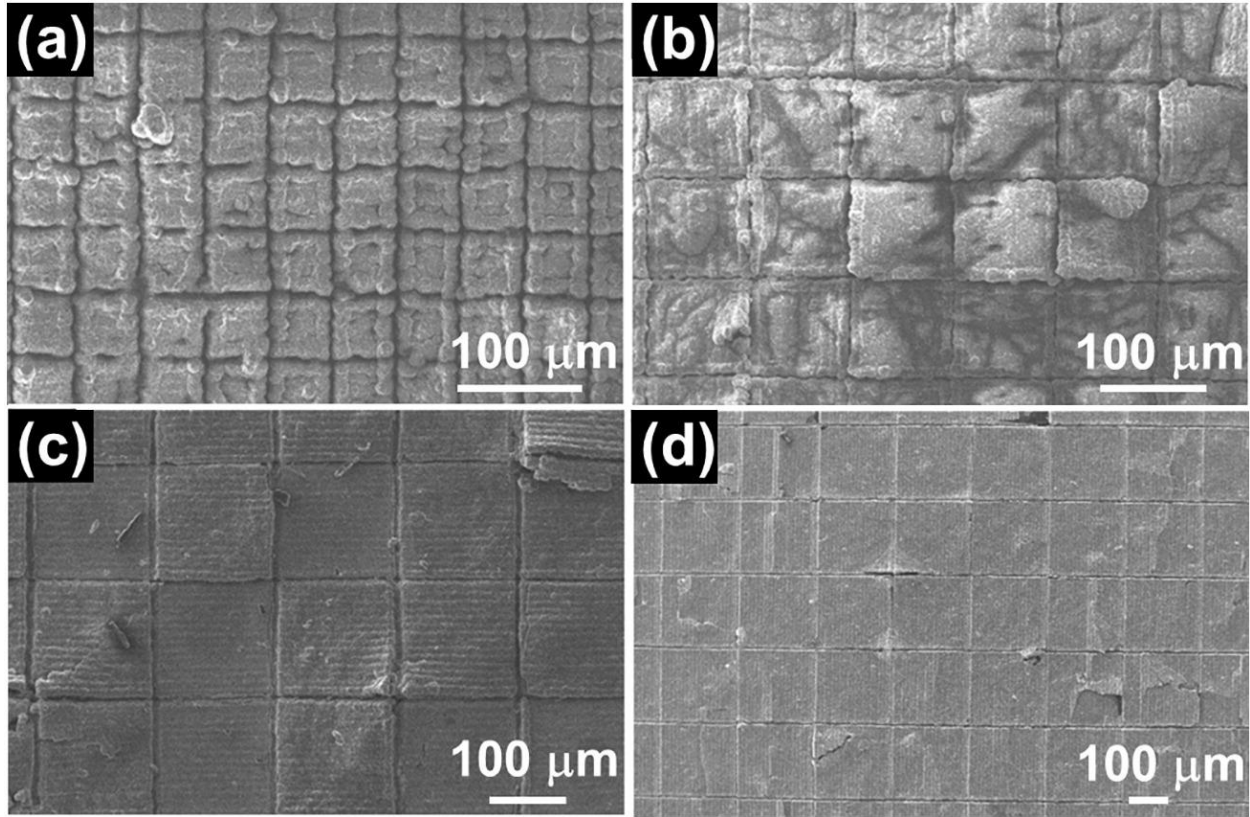


**Figure 7.** SEM images of diamond films grown on fs-laser-scribed Cu surfaces with grid sizes of (a) 50, (b) 100, (c) 150, and (d) 200  $\mu\text{m}$ .